

## Direct Measurement of Heavy-Hole Exciton Transport in Type-II GaAs/AlAs Superlattices

G. D. Gilliland,<sup>1</sup> A. Antonelli,<sup>1</sup> D. J. Wolford,<sup>2</sup> K. K. Bajaj,<sup>1</sup> J. Klem,<sup>3</sup> and J. A. Bradley<sup>2</sup>

<sup>1</sup>Department of Physics, Emory University, Atlanta, Georgia 30322

<sup>2</sup>IBM T.J. Watson Research Center, P.O. Box 218, Yorktown Heights, New York 10598

<sup>3</sup>Sandia National Laboratories, Albuquerque, New Mexico 87185

(Received 4 August 1993)

We have directly measured the transport of heavy-hole excitons in a type-II GaAs/AlAs superlattice. Our results constitute the first direct confirmation of exciton localization in type-II structures and thermal activation to more mobile states. We have also developed a quantitative model to explain our transport and kinetics results, and have obtained the nonradiative interfacial defect density.

PACS numbers: 78.47.+p, 68.65.+g, 71.35.+z, 72.80.Ey

Band-structure engineering of semiconductor materials may drastically change the optical and electronic properties from those normally observed in the bulk depending on whether electrons and holes are confined in the same layer (type-I superlattices and quantum wells) or in different layers (type-II superlattices) [1–4]. For type-II superlattices, these structure-induced changes may enhance certain processes, including real-space transfer, spatially indirect recombination, excitonic localization, and carrier scattering at heterointerfacial potential fluctuations [5–10]. In spite of these studies, a quantitative understanding of exciton kinetics in type-II structures is still lacking. Additionally, characterization of excitonic transport properties has been problematical due to their electrical neutrality which precludes the use of conventional electrical transport techniques.

For the (GaAs)<sub>m</sub>/(AlAs)<sub>n</sub> system, type-II band alignment results for GaAs-layer thicknesses < 35 Å ( $m < 13$ ) and AlAs-layer thicknesses > 15 Å ( $n > 6$ ) [3] or through the application of hydrostatic pressure [9]. In such structures, the hole ground state is in the GaAs layer (at the  $\Gamma$  point), whereas, in contrast, the nature of the electronic ground state has been disputed [5–8]. This difficulty has arisen due to the lifting of the threefold degeneracy of  $X$ -electron states in the AlAs layers by several processes, including strain-induced splitting of  $X_Z$  and  $X_{X,Y}$ , electronic mass anisotropy [ $m_e(X_Z) = 1.1m_0$  and  $m_e(X_{X,Y}) = 0.19m_0$ ],  $\Gamma$ - $X$  mixing due to the superlattice potential near  $\Gamma$ - $X$  crossing, and interface disorder induced potential fluctuations [5–8,11]. Nevertheless, there is agreement that the universally observed rapid decrease in photoluminescence (PL) lifetime with increasing temperature results from thermal activation from localized states. *However, this has never been shown experimentally.*

In this Letter we report, to our knowledge, the *first* direct experimental determination of excitonic transport in type-II superlattices, specifically, GaAs/AlAs short-period superlattices. Additionally, we have quantitatively modeled the temperature dependence of both the exciton kinetics and transport. We *demonstrate directly* that the transport is governed by the thermal activation from lo-

calized states to highly mobile states. Furthermore, we quantify the interfacial nonradiative defect density and the heterointerfacial disorder that is most probably responsible for the observed excitonic localization.

In order to measure excitonic transport we have resorted to an all-optical analog of the classic Haynes-Shockley experiment, whereby excitonic PL is spatially and temporally resolved [12]. There are several varieties of this basic technique, and ours relies on confocal laser excitation and imaging of the photoexcited excitons. PL was excited by a synchronously pumped cavity-dumped dye laser (1 ps pulse width) pumped by a frequency-doubled cw mode-locked Nd<sup>3+</sup>:YAG laser. With this experimental arrangement, near diffraction-limited laser spot sizes ( $\sim 3 \mu\text{m}$ ) are achievable, with a temporal and spectral resolution of  $\sim 50$  ps and  $\sim 0.1$  meV, respectively.

The sample used in this study was an undoped molecular-beam-epitaxy-prepared (GaAs)<sub>11</sub>/(AlAs)<sub>19</sub> superlattice with 55 periods. GaAs layers are 30 Å thick and AlAs layers are 50 Å thick. Most studies [5,6] have concluded that the lowest electronic bound state is  $X_Z$  for thin structures, whereas for superlattices with AlAs barriers > 60 Å thick the lowest state is  $X_{X,Y}$ . Jaros and co-workers [13] have found that  $X_Z$  is the ground state regardless of the structure. Thus, the prevailing view is that  $X_Z$  is the electronic ground state of our structure.

Figure 1 shows the cw PL spectra versus temperature from 2 to 30 K. The  $X_Z$ - $\Gamma$  no-phonon line is clearly evident and the lower-energy phonon replicas are much weaker. These cw spectra show the remarkable temperature invariant PL line shape of the  $X_Z$ - $\Gamma$  no-phonon line—with no shift in peak emission energy, very little broadening of the PL line, and a small decrease in emission intensity. With pulsed excitation (at a repetition rate slower than the longest decay time) we find that the PL intensity decreases by  $> 10^3$  while the line shape again remains invariant. The linewidth of the  $X_Z$ - $\Gamma$  no-phonon line is  $\sim 5.5$  meV at 1.8 K and only increases to  $\sim 5.8$  meV at 30 K, whereas  $kT$  at 30 K is 2.6 meV.

Figure 2 shows PL time decays versus temperature for the  $X_Z$ - $\Gamma$  no-phonon line. At low temperatures the decays are nonexponential and very slow, whereas for in-

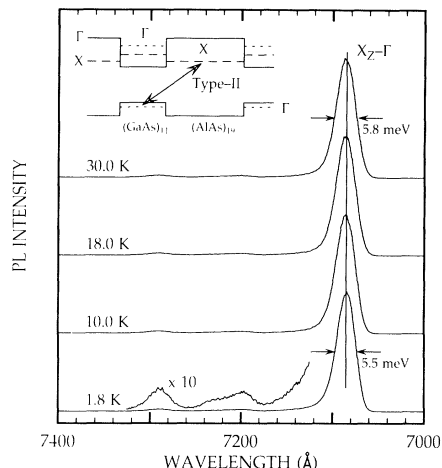


FIG. 1. PL spectra versus temperature after cw excitation at 4579 Å. All spectra are normalized. Inset shows  $X_Z\text{-}\Gamma$  phonon transition.

creasing temperature the decays become exponential (over 3 decades) and much faster. These decays may be quantified by their lifetimes deduced from the long-time exponential tail of the decays—yielding lifetimes ranging from  $\sim 21 \mu\text{s}$  at 1.8 K to  $\sim 15 \text{ ns}$  at 30 K.

Using our time-resolved confocal PL-imaging technique, we have obtained the time-dependent spatial profile of the radiating carriers. We observe a systematic expansion of the luminescence from the initial laser spot size of  $\sim 5 \mu\text{m}$  to over  $30 \mu\text{m}$  at high temperatures. We find, under our excitation conditions ( $< 10^{12}$  photons/ $\text{cm}^2$ ), that the transport is diffusive, with diffusion coefficients versus temperature shown in Fig. 3. There is a  $> 10^3$  increase of diffusion constant,  $D$ , with temperature—from  $\sim 2 \times 10^{-3} \text{ cm}^2/\text{s}$  at 1.8 K to  $\sim 7 \text{ cm}^2/\text{s}$  at 30 K. An Arrhenius plot of the diffusion constant yields an activation energy of  $\sim 6.8 \pm 1.5 \text{ meV}$ .

Based upon PL kinetics alone, most reports [4,8] have concluded that the temperature dependence arises from the thermally activated detrapping of excitons from localized states to mobile states. However, this hypothesis has never been proven since the spatial transport of these excitons has never been measured. Our results demonstrate the temperature-dependent transport of these excitons, which is crucial to this localization model. Furthermore, the observed temperature-independent PL line shapes suggest that the type-II radiative recombination only occurs from localized states; otherwise, the excitonic recombination from the higher-energy mobile states would yield a distinct high-energy tail in the PL spectra. Since spatially separated electrons and holes are in intimate contact with the heterointerface due to their mutual Coulomb attraction, their optical properties should be very sensitive to any possible heterointerfacial disorder. Thus, we conclude that the localization most probably results from heterointerfacial disorder, and that this is vital

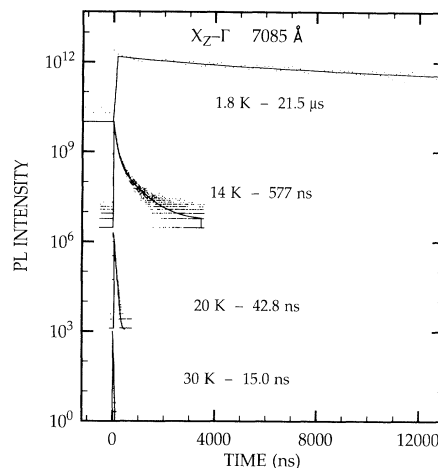


FIG. 2.  $X_Z\text{-}\Gamma$  PL decay kinetics versus temperature after pulsed excitation at 6000 Å.

to the recombination mechanism. The PL spectrum (line shape) is indicative of the distribution of localized states. Recent theoretical work has confirmed the role of interface localization in the PL spectra of various systems [14]. Also, our results suggest that the mobile states are  $\sim 6.8 \pm 1.5 \text{ meV}$  higher in energy than the distribution of localized states.

The observed transport probably results from the temperature-dependent excitonic occupation of mobile versus stationary localized states, rather than from a temperature dependence of the mobile exciton diffusivity alone. We may thus extend the previously proposed model as follows: (1) At low temperatures all excitons are localized and the PL is indicative of this localized state distribution. (2) As temperature is increased excitons may be thermally detrapped into the mobile states. (3) These mobile excitons may then spatially diffuse, without radiating. (4) As these mobile excitons diffuse they may become trapped at a nonradiative defect. (5) The mobile

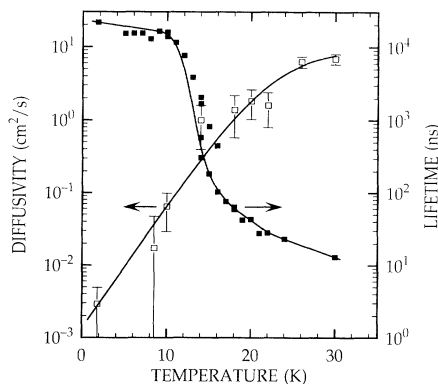


FIG. 3. Temperature dependence of diffusivity and lifetimes derived from our transport and PL decay kinetics measurements.

excitons may spatially diffuse, become relocated in the lower-energy sites, and subsequently recombine. This model explains all the experimental observations.

Based on the premises above and using as a starting point the theory by Chandrasekhar [15] treating coagulation in colloids, we developed a quantitative model to compare with our experimental results. Here, we divide the photoexcited 2D excitonic population into two categories, localized  $n_l$  and mobile  $n_m$  ( $N = n_l + n_m$ ), where the relative populations are related by an Arrhenius

term  $\exp(-\Delta E_a/kT)$ . The mobile population is free to diffuse, and possibly becomes trapped at a perfectly absorbing nonradiative defect. We have solved the diffusion equation for the mobile excitons in 2D using the Wigner-Seitz method [16] with the following boundary conditions:  $n_m = C_0$  at  $t=0$ , and  $n_m = 0$  at  $r = r_1$ ,  $\partial n_m / \partial r = 0$  at  $r = r_2$  for  $t \geq 0$ , where  $r_1$  is the radius of the perfectly absorbing defect and  $2r_2$  is the mean separation between defects. This yields the time-dependent density of mobile excitons

$$n_m(t) = \frac{\pi^2 C_0 r_1}{2} \sum_{n=1}^{\infty} \left[ \frac{\alpha_n J_0^2(\alpha_n r_1)}{J_0^2(\alpha_n r_1) - J_1^2(\alpha_n r_2)} \right] \{Y_1(\alpha_n r_2) J_1(\alpha_n r_1) - J_1(\alpha_n r_2) Y_1(\alpha_n r_1)\} U(\alpha_n r) e^{-D \alpha_n^2 t}, \quad (1)$$

where  $U(\alpha_n r) = Y_1(\alpha_n r_2) J_0(\alpha_n r) - J_1(\alpha_n r_2) Y_0(\alpha_n r)$ , and  $\alpha_n$  are the zeros of  $U(\alpha_n r)$ . Here,  $J_i$  and  $Y_i$  ( $i=0,1$ ) are the Bessel and modified Bessel functions of order  $i$ . Using the Klein-Sturge-Cohen (KSC) theory [17] for radiative decay in an alloy (distribution of radiative rates), which approximates the heterointerface disorder induced randomness in this type-II excitonic system (although the exact shape of this distribution is unknown), the PL decay kinetics may be modeled as

$$I(t) = I_0 \exp\left(-\int_0^t w_{nr} dt'\right) (1 + e^{-w_r t})^{-3/2}, \quad (2)$$

where

$$w_{nr}(t) = \frac{-2\pi D r_1 (\partial n_m(r,t) / \partial r)|_{r=r_1}}{2\pi \int_{r_1}^{r_2} n_m(r,t) r dr}, \quad (3)$$

and  $w_r$  and  $w_{nr}$  are the radiative and nonradiative rates, respectively.

We have derived a microscopic model for nonradiative decay in type-II superlattices, thus extending the KSC theory to specifically model this process. Figure 4 shows

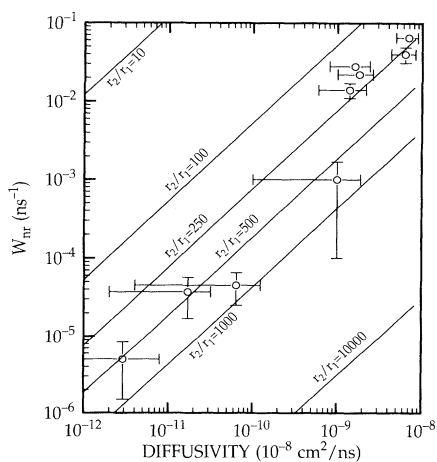


FIG. 4. Comparison of calculated nonradiative decay rates versus diffusivity and experimentally determined values. The best fit is obtained for  $r_2/r_1 \approx 250$ .

results of our model calculation compared with our experimental measurements, using only  $r_1$  and  $r_2$  as adjustable parameters. We find good agreement between experiment and theory for  $r_1 = 115 \text{ \AA}$  and  $r_2 = 2.9 \text{ \mu m}$ . This implies a nonradiative defect sheet density of  $\sim 1.2 \times 10^7 \text{ cm}^{-2}$ . We have assumed that  $r_1$  is equal to the 2D exciton Bohr radius [18]. This nonradiative defect density is also consistent with the temperature-independent diffusion lengths of  $\sim 3 \text{ \mu m}$  derived from our transport and kinetic measurements. This relatively small density of nonradiative defects is consistent with possible heterointerfacial oxygen incorporation and/or interfacial dislocations [19], but this is only speculation.

One possible explanation for the electronic energy-level system deduced from these measurements might be due to the nondegenerate  $X_Z$  and  $X_{X,Y}$  states. Excitons in the lower energy  $X_Z$  state, with momentum perpendicular to the layer, may be localized, whereas excitons in the  $X_{X,Y}$  states, with momentum parallel to the layer and in the plane of observation, may lie  $\sim 7 \text{ meV}$  higher in energy and be highly mobile. We also recognize that our experiments actually excite excitons at all interfaces, and thus our diffusion constants, nonradiative trap densities, etc., are indicative of an average over all interfaces.

In summary, we report here a direct observation of the heretofore only postulated temperature-dependent, spatial localization of cross-interface excitons in type-II superlattices. We have also developed a quantitative model relating the excitonic decay kinetics to their transport. Our model accurately predicts the observed PL decay kinetics using the measured diffusivities. From this model we may characterize the heterointerface quality in terms of the density of nonradiative traps, which for this sample is about  $1.2 \times 10^7 \text{ cm}^{-2}$ .

This work was supported in part by ONR under Contracts No. N00014-90-C-0077 and No. N00014-92-J-1927, and AFOSR under Grant No. AFOSR-91-0056.

[1] R. Dingle, A. C. Gossard, and W. Wiegmann, Phys. Rev. Lett. **34**, 1327 (1975).

- [2] A. C. Gossard, P. M. Petroff, W. Weigmann, R. Dingle, and A. Savage, *Appl. Phys. Lett.* **29**, 323 (1976).
- [3] E. Finkman, M. D. Sturge, M. H. Meynadier, R. E. Nahory, M. C. Tamargo, D. M. Hwang, and C. C. Chang, *J. Lumin.* **39**, 57 (1987).
- [4] B. A. Wilson, *IEEE J. Quantum Electron.* **24**, 1763 (1988).
- [5] W. Ge, M. D. Sturge, W. D. Schmidt, L. N. Pfeiffer, and K. W. West, *Appl. Phys. Lett.* **57**, 55 (1990).
- [6] H. W. van Kesteren, E. C. Cosman, P. Dawson, K. J. Moore, and C. T. Foxon, *Phys. Rev. B* **39**, 13426 (1989).
- [7] F. Minami, K. Hirata, K. Era, T. Yao, and Y. Masumoto, *Phys. Rev. B* **36**, 2875 (1987).
- [8] J. Ihm, *Appl. Phys. Lett.* **50**, 1068 (1987).
- [9] T. W. Steiner, D. J. Wolford, T. F. Kuech, and M. Jaros, *Superlattices Microstruct.* **4**, 227 (1988).
- [10] J. Feldmann, R. Sattmann, E. O. Göbel, J. Kuhl, J. Hebling, K. Ploog, R. Muralidharan, P. Dawson, and C. T. Foxon, *Phys. Rev. Lett.* **62**, 1892 (1989).
- [11] T. J. Drummond, E. D. Jones, H. P. Hjalmarson, and B. L. Doyle, *Proc. SPIE Int. Soc. Opt. Eng.* **796**, 2 (1987).
- [12] G. D. Gilliland, D. J. Wolford, T. F. Kuech, and J. A. Bradley, *Appl. Phys. Lett.* **59**, 216 (1991); D. J. Wolford, G. D. Gilliland, T. F. Kuech, J. A. Bradley, and H. P. Hjalmarson, *Phys. Rev. B* **47**, 15601 (1993).
- [13] L. D. L. Brown, M. Jaros, and D. J. Wolford, *Phys. Rev. B* **40**, 6413 (1989).
- [14] M. Jaros and A. W. Beavis, *Appl. Phys. Lett.* **63**, 669 (1993).
- [15] S. Chandrasekhar, *Rev. Mod. Phys.* **15**, 1 (1943).
- [16] M. Muskat, *The Flow of Homogeneous Fluids Through Porous Media* (McGraw-Hill, New York, 1937).
- [17] M. V. Klein, M. D. Sturge, and E. Cohen, *Phys. Rev. B* **25**, 4331 (1982).
- [18] J. Cen, S. V. Branis, and K. K. Bajaj, *Phys. Rev. B* **44**, 12848 (1991).
- [19] M. T. Asom, M. Geva, R. E. Leibenguth, and S. N. G. Chu, *Appl. Phys. Lett.* **59**, 976 (1991).